JOURNAL OF MAGNETIC RESONANCE 58, 370–388 (1984)

Selection of Coherence-Transfer Pathways in NMR Pulse Experiments

GEOFFREY BODENHAUSEN, HERBERT KOGLER,* AND R. R. ERNST

Laboratorium für Physikalische Chemie, Eidgenössische Technische Hochschule, 8092 Zurich, Switzerland

Received September 29, 1983; revised December 13, 1983

NMR pulse experiments are described in terms of pathways through various orders of coherence. A general procedure is indicated for the systematic design of phase cycles that select desirable coherence-transfer pathways.

INTRODUCTION

Some of the most successful new pulse techniques in high-resolution nuclear magnetic resonance rely on coherence-transfer processes. To name a few, we mention homonuclear and heteronuclear two-dimensional (2D) correlation spectroscopy (*1–7*), multiple-quantum spectroscopy (*8–12*), multiple-quantum filtering (*13–16*), spin pattern recognition (*17*), and various methods for the enhancement and simplification of 1D carbon-13 spectra (*18–21*). The development of these experiments has been accompanied by a proliferation of recipes for the elimination of unwanted signals and artifacts by phase-cycling techniques. Because many different, often rather intuitive approaches have been used, the common basis of these techniques is not always transparent.

In an effort to provide a unified picture, we describe pulse experiments in terms of pathways through various orders of coherence. This "coherence-transfer pathway" approach turns out to be useful to design novel experiments for specific purposes. The selection of the desired pathway is accomplished experimentally by means of phase-cycling procedures.

There are parallels between this work and a paper recently submitted by A. D. Bain (*22*), who also applied the concept of coherence-transfer pathways. In the present paper, we demonstrate its utility in homonuclear experiments involving several coherence-transfer steps, while Bain is concerned with the systematic description of phase cycles in connection with quadrature detection and heteronuclear coherence transfer (*22*).

COHERENCE AND COHERENCE-TRANSFER PATHWAYS

The concept of "coherence" is a generalization of the notion of transverse magnetization. Coherence can be associated with a transition between a pair of eigenstates

* Present address: Institut für Organische Chemie, Universität Frankfurt, D-6000 Frankfurt, West Germany.

0022-2364/84 $3.00

$|r\rangle$ and $|s\rangle$ with an arbitrary difference in magnetic quantum numbers $p_{rs} = M_r - M_s$. Transverse magnetization corresponds to a particular class of coherence associated with a change in quantum number $p = \pm 1$.

Formally, coherence can be conceived as a coherent superposition of two eigenstates (*23*)

$$\psi_{rs} = a_r|r\rangle + a_s|s\rangle. \qquad [1]$$

Such a non-equilibrium state develops in time under the time-independent free precession Hamiltonian. In terms of the density operator σ, coherence between the states $|r\rangle$ and $|s\rangle$ is expressed by the existence of nonzero density matrix elements $\sigma_{rs} = |r\rangle\langle s|$ and $\sigma_{sr} = |s\rangle\langle r|$. These elements indicate a "transition in progress" between the two connected states.

In high-field NMR, each eigenstate $|r\rangle$ is characterized by a magnetic quantum number M_r and each coherence σ_{rs} by a magnetic quantum number difference $p_{rs} = M_r - M_s$ which we call "coherence order." Note that each transition is associated with two coherences σ_{rs} and σ_{sr} with coherence orders of opposite sign. The quantities M_r and p_{rs} are "good" quantum numbers,[1] and each coherence σ_{rs} conserves its quantum number p_{rs} in the course of free precession. Radiofrequency (rf) pulses, however, may induce a transfer between coherences σ_{rs} and σ_{tu}, a process that may change the coherence order.

It is often sufficient to classify the various terms of the density operator according to the coherence order p:

$$\sigma(t) = \sum_p \sigma^p(t). \qquad [2]$$

For a system of K spins 1/2, p extends from $-K$ to K. This classification can be carried out explicitly if the density operator is expressed in matrix elements, or alternatively in a suitable set of base operators, such as irreducible tensor operators T_{lp} (*24*), products of shift operators (e.g., $I_k^+ I_l^+$) (*25*), or single-transition shift operators (e.g., $I^{+(rs)} = I_x^{(rs)} + iI_y^{(rs)}$). On the other hand, products of Cartesian operators (e.g., $I_{kx}I_{lx}$) (*25*) or Cartesian single-transition operators $I_x^{(rs)}$ (*26, 27*) are not particularly suitable for a classification according to p.

The characteristic properties of coherence of order p (or simply "p-quantum coherence") are demonstrated by the transformation under rotations about the z axis:

$$\exp\{-i\varphi F_z\}\sigma^p \exp\{i\varphi F_z\} = \sigma^p \exp\{-ip\varphi\} \qquad [3]$$

where

$$F_z = \sum_{k=1}^{N} I_{kz}.$$

We found it convenient to represent the sequence of events in various experiments in a "coherence transfer map" such as shown in Fig. 1. Free precession proceeds within the levels of this map, while pulses may induce "transitions" between coherence

[1] This is related to the fact that the Hamiltonian has rotational symmetry. The eigenstate $|r\rangle$ transforms according to the irreducible representation M_r of the one-dimensional rotation group (*24*). Hence $|r\rangle\langle s|$ transforms according to the representation $p_{rs} = M_r - M_s$.

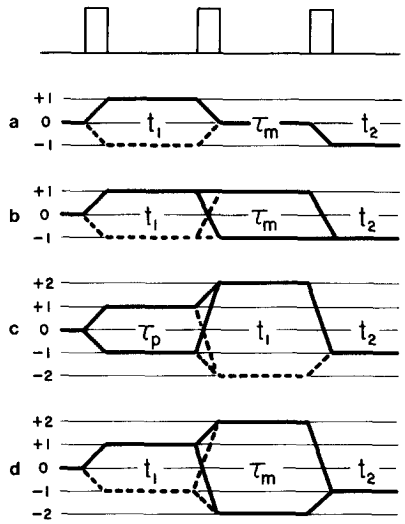

FIG. 1. Coherence-transfer maps (CT maps) for various 2D experiments involving three pulses. Solid lines indicate pathways that involve a single-order p in the evolution period. For a basic understanding of the experiments, these pathways suffice. If pure phase lineshapes are not essential (e.g., if composite lineshapes or absolute-value plots are acceptable), it is sufficient to select the pathways shown by solid lines. Mirror-image pathways with $-p$ in t_1 are indicated by dashed lines. For pure phase spectra (i.e., pure 2D absorption lineshapes), both solid and dashed pathways must be retained. Four experimental schemes are shown: (a) 2D exchange spectroscopy (NOESY), (b) relayed correlation spectroscopy (pathways shown for fixed mixing interval τ_m), (c) double-quantum spectroscopy and (d) 2D correlation spectroscopy with double-quantum filter ($\tau_m = 0$).

orders. The route of a particular component of coherence is referred to as a "coherence-transfer pathway." All coherence-transfer pathways of a pulse experiment start with $p = 0$ (thermal equilibrium) and must end with single-quantum coherence to be detectable. If we choose to observe the complex signal in the detection interval by quadrature detection,

$$s^+(t) = s_x(t) + is_y(t) = \mathrm{Tr}\{\sigma(t)F_x\} + i\,\mathrm{Tr}\{\sigma(t)F_y\} = \mathrm{Tr}\{\sigma(t)F^+\} \qquad [4]$$

where $F^+ = \sum_k I_k^+$, only density operator components proportional to I_k^- can contribute to the signal, and all pathways that do not lead to $p = -1$ can be disregarded. However, as noted by Bain (*22*), imperfect quadrature detection (i.e., imbalance of the two receiver channels) leads to partial observation of single-quantum coherence components with $p = +1$.

The examples in Fig. 1 show the coherence transfer pathways that are relevant to four well known techniques involving three consecutive coherence-transfer steps. Apart from the incrementation of the intervals in the course of the experimental sequence, these methods merely differ in the selection of coherence-transfer pathways. A single pathway suffices if absolute-value spectra or phase-sensitive spectra with composite ("phase-twisted") lineshapes are acceptable, while "mirror image" pathways (dashed lines in Fig. 1) must be retained simultaneously if pure phase spectra (i.e., pure 2D absorption lineshapes) are essential, as will be discussed below.

It is important to note that the order $p = 0$ may comprise Zeeman polarization (represented by density operator terms proportional to I_{kz}), longitudinal scalar or dipolar spin order (e.g., $I_{kz}I_{lz}$), and zero-quantum coherence (e.g., $I_k^+I_l^-$). This is particularly relevant for 2D exchange spectroscopy (Fig. 1a) (*28, 29*). In the case of relayed magnetization transfer (Fig.1b) (*30*) the delay τ_m can be kept constant, in which case the sign of the coherence order in τ_m is irrelevant and two pathways can be allowed simultaneously. It is also possible to vary τ_m in concert with t_1 (*31, 32*), in which case the pathway selection determines whether the ω_1 domain will contain sums or differences of chemical shifts. In multiple-quantum spectroscopy (Fig. 1c) (*8–12*), we have the option of observing both $+p$ and $-p$ coherences in the evolution period, or we may restrict the transfer as shown by solid lines. In correlation spectroscopy with multiple-quantum filters (Fig. 1d) (*14*), it is not necessary to select the sign of the coherence order in the τ_m interval, but one has the option of selecting only $p = +1$ coherence in the evolution period.

SELECTION OF COHERENCE-TRANSFER PATHWAYS

In experiments employing nonselective pulses, numerous coherence-transfer pathways can occur simultaneously. In principle, it is possible to use cascades of selective pulses to restrict the number of pathways, but it turns out that phase-shifted nonselective pulses provide a more flexible approach to the selection of desirable pathways.

Consider a complete pulse experiment with n coherence transfer processes expressed by the propagators $U_1, U_2, \cdots U_n$:

$$\sigma_0 \xrightarrow{U_1} \xrightarrow{U_2} \cdots \xrightarrow{U_n} \sigma(t). \qquad [5]$$

In the context of 2D spectroscopy, the first propagator typically represents the excitation process, while the last propagator corresponds to the conversion into observable magnetization. The intermediate propagators, which only occur in some experiments, induce coherence transfer between various orders. A propagator may represent a single pulse or a sequence of pulses, such as the composite sequence $(\pi/2)$–τ–(π)–τ–$(\pi/2)$ commonly used for multiple-quantum excitation (*25*). Each propagator U_i causes a transfer of a particular order of coherence $\sigma^p(t_i^-)$ into numerous different orders $\sigma^{p'}(t_i^+)$:

$$U_i\sigma^p(t_i^-)U^{-1} = \sum_{p'} \sigma^{p'}(t_i^+) \qquad [6]$$

where the arguments of the density operators refer to the state just before and immediately after the transformation by U_i. This leads to a "branching" or "fanning out" of the coherence-transfer pathways. After n consecutive coherence-transfer steps, each pathway can be characterized by a set of n values:

$$\Delta p_i = p'(t_i^+) - p(t_i^-) \qquad [7]$$

corresponding to the changes in coherence order under the propagators U_i. The complete pathway is therefore specified by a vector

$$\mathbf{\Delta p} = \{\Delta p_1, \Delta p_2, \ldots, \Delta p_n\}. \qquad [8]$$

Since all pathways must begin with $p = 0$ and are assumed to end with $p = -1$ to be observable (see Eq. [4]), the sum of the components of the vector $\mathbf{\Delta p}$ is fixed,

$$\sum_i \Delta p_i = -1. \qquad [9]$$

Thus if $(n - 1)$ values of Δp_i are specified by $(n - 1)$ independent phase cycles as discussed below, the entire vector $\mathbf{\Delta p}$ and hence the complete pathway are defined unambiguously. Because the rf phase shifts required for the pathway selection are often subject to systematic errors, it may however be advisable in practice to employ n independent phase cycles to select the desired Δp_i values under *all* n coherence transfer steps.

The key to the separation of coherence-transfer pathways is the use of propagators $U_i(\varphi_i)$ that are shifted in phase

$$U_i(\varphi_i) = \exp\{-i\varphi_i F_z\} U_i(0) \exp\{i\varphi_i F_z\}. \qquad [10]$$

If a particular propagator U is made up of a sequence of pulses, each constituent pulse must be incremented in phase. For example, the excitation sequence commonly used in double-quantum spectroscopy becomes $(\pi/2)_\varphi$–τ–$(\pi)_\varphi$–τ–$(\pi/2)_\varphi$.

Under a phase-shifted propagator $U_i(\varphi_i)$, Eq. [6] takes the form

$$U_i(\varphi_i)\sigma^p(t_i^-)U(\varphi_i)^{-1} = \sum_{p'} \sigma^{p'}(t_i^+) \exp\{-i\Delta p_i \varphi_i\}. \qquad [11]$$

Thus the phase shift of a coherence component that is transferred by the propagator U_i is given by $\Delta p_i \varphi_i$. In symbolic notation, Eq. [11] may be written

$$\sigma^p(t_i^-) \xrightarrow{U_i(\varphi_i)} \sum_{p'} \sigma^{p'}(t_i^+) \exp\{-i\Delta p_i \varphi_i\}. \qquad [12]$$

After n consecutive coherence-transfer steps, one obtains single-quantum coherence components ($p = -1$) with phases that reflect the pathways $\mathbf{\Delta p}$ and the propagator phases φ_i:

$$\sigma^{p=-1}(\varphi_1, \varphi_2, \ldots, \varphi_n, t) = \sigma^{p=-1}(\varphi_1 = \varphi_2 = \cdots = \varphi_n = 0, t)$$
$$\times \exp\{-i(\Delta p_1\varphi_1 + \Delta p_2\varphi_2 + \cdots + \Delta p_n\varphi_n)\} \qquad [13a]$$
$$= \sigma^{p=-1}(\boldsymbol{\varphi} = \mathbf{0}) \exp\{-i\mathbf{\Delta p}\boldsymbol{\varphi}\} \qquad [13b]$$

with the vector notation for $\mathbf{\Delta p}$ in Eq. [8] and

$$\boldsymbol{\varphi} = \{\varphi_1, \varphi_2, \ldots, \varphi_n\}. \qquad [14]$$

The phase shifts of Eq. [13] also occur in the complex signal observed during the detection period (Eq. [4]). It is convenient to decompose the signal into contributions of individual pathways:

$$s(t) = \sum_{\mathbf{\Delta p}} s^{\mathbf{\Delta p}}(t). \qquad [15]$$

With a given vector of phase shifts $\boldsymbol{\varphi}$, the signal associated with a certain pathway carries the phase

$$s^{\mathbf{\Delta p}}(\boldsymbol{\varphi}, t) = s^{\mathbf{\Delta p}}(\mathbf{0}, t) \exp\{-i\mathbf{\Delta p}\boldsymbol{\varphi}\}. \qquad [16]$$

The characteristic phase shift in Eq. [16] can be used, following Wokaun and Ernst (*9*), to separate the different pathways under a particular propagator U_i by a Fourier analysis with respect to the rf phase of this propagator U_i.

To restrict the coherence transfer under U_i to a particular change Δp_i in coherence order, we may perform N_i experiments where the rf phase φ_i of the propagator is incremented systematically:

$$\varphi_i = k_i 2\pi/N_i, \qquad k_i = 0, 1, \ldots, N_i - 1. \qquad [17]$$

The N_i signals $s(\varphi_i, t)$ observed in the detection period are then combined according to a discrete Fourier analysis with respect to the phase φ_i,

$$s^{\Delta p_i}(t) = \frac{1}{N_i} \sum_{k_i=0}^{N_i-1} s(\varphi_i, t) \exp(i\Delta p_i \varphi_i). \qquad [18]$$

By this process, all coherence-transfer pathways are selected which undergo a change in coherence order Δp_i under the propagator U_i. However, by carrying out a series of N_i experiments, it is not possible to select a unique Δp_i, but rather a series of values $\Delta p_i \pm nN_i$ with $n = 0, 1, 2, \ldots$. This situation is reminiscent of aliasing in Fourier analysis and is a consequence of the sampling theorem. Clearly, if a unique Δp_i value must be selected from a range of r consecutive values, N_i must be chosen at least equal to r.

It is useful to exhibit the required selectivity of the phase cycle by listing all possible changes in coherence order, for example,

$$\Delta p_i\colon -3, -2, \mathbf{-1}, (0), (1), 2, 3, \qquad [19]$$

where the values of Δp_i that must be blocked are set in parentheses, while the desired value is set in boldface. The minimum number of experiments to be performed in this case would be $N_i = 3$. The examples discussed below will illustrate the resulting phase cycles.

In many experiments a more restrictive selection of pathways is desired than can be obtained by cycling the phase of a single propagator U_i. In such cases, a desired pathway with successive changes in coherence order $\Delta p_1, \Delta p_2, \ldots, \Delta p_n$ under the n propagators can be retained selectively by cycling the phases of each of the relevant propagators $U_1(\varphi_1), U_2(\varphi_2), \ldots, U_n(\varphi_n)$ separately:

$$\varphi_1 = k_1 2\pi/N_1, \ldots, \qquad \varphi_n = k_n 2\pi/N_n,$$

for

$$k_1 = 0, 1, \ldots, N_1 - 1, \ldots, \qquad k_n = 0, 1, \ldots, N_n - 1. \qquad [20]$$

A unique prescription for the phase cycle is obtained by incrementing k_1 through all N_1 steps before incrementing k_2. The total number of experiments to be performed is determined by the product $N = N_1 \cdot N_2 \cdot \ldots \cdot N_n$. To select the desired pathway characterized by the vector $\mathbf{\Delta p}$ in Eq. [8], the signals must be combined according to

$$s^{\Delta p}(t) = \frac{1}{N} \sum_{k_1=0}^{N_1-1} \sum_{k_2=0}^{N_2-1} \cdots \sum_{k_n=0}^{N_n-1} s(t) \exp\{+i\mathbf{\Delta p \varphi}\} \qquad [21]$$

where

$$\mathbf{\Delta p \varphi} = \Delta p_1 k_1 2\pi/N_1 + \Delta p_2 k_2 2\pi/N_2 + \cdots + \Delta p_n k_n 2\pi/N_n. \qquad [22]$$

The principle of the pathway selection becomes obvious by observing that the signal $s(t)$ consists of the contributions of all possible pathways $\Delta\mathbf{p}'$ (see Eqs. [15] and [16]):

$$s(t) = \sum_{\Delta\mathbf{p}'} s^{\Delta\mathbf{p}'}(\mathbf{0}, t) \exp\{-i\Delta\mathbf{p}'\boldsymbol{\varphi}\}. \qquad [23]$$

Clearly, the discrete n-dimensional Fourier analysis in Eq. [21] leads to a nonvanishing signal for $\Delta\mathbf{p}' = \Delta\mathbf{p}$. However, since the selectivity under each propagator U_i is determined by the number N_i of phase increments, there are a manifold of pathways that survive the selection process, with

$$\Delta\mathbf{p} = \{\Delta p_1 \pm n_1 N_1, \Delta p_2 \pm n_2 N_2, \ldots, \Delta p_n \pm n_n N_n\}. \qquad [24]$$

Because the maximum order of coherence $|p_{\max}| \leqslant K$ in a system with K spins 1/2, and because the amplitude of coherence transfer into very high orders is small, it is usually possible to retain a unique pathway by relatively small increment numbers N_i.

There are three different strategies to achieve the multiplication of the signals by the phase factors necessary for the Fourier analysis in Eq. [21]: (a) multiplication of the complex signals with complex phase factors (this can be achieved conveniently with routine phase-correction procedures); (b) phase-shifting of all pulses in the sequence through $\Sigma\, \Delta p_i \varphi_i$ and addition of the signals without weighting; (c) shifting of the phase of the receiver reference channel. Strategy (c) was adopted in the experimental examples discussed below. With the definition of the observable operator F^+ in Eq. [4], the reference phase must be $\varphi^{\text{ref}} = -\Sigma\, \Delta p_i \varphi_i$. The opposite phase shift must be applied if the observable operator is F^-, in which case the pathways terminate at the level $p = +1$.

The parameters involved in Eq. [21] are shown schematically in Fig. 2 for a hypothetical experiment involving three coherence-transfer steps. To select the desired pathway, the reference channel of the phase-sensitive detector (PSD) can be shifted in phase as indicated in the figure.

PURE 2D ABSORPTION LINESHAPES

In the evolution period t_1, there are always two coherences associated with each transition $|r\rangle \leftrightarrow |s\rangle$ that have opposite orders $p = M_r - M_s$ and $p' = -p$ and opposite frequencies. If the two coherence-transfer pathways $+p \rightarrow -1$ and $-p \rightarrow -1$ are both allowed, the counterrotating components lead, after complex Fourier transformation with respect to t_1, to signals that are symmetrically disposed about $\omega_1 = 0$. Each signal has a lineshape that consists of an admixture of 2D absorption and 2D dispersion components (*1*). This composite lineshape is often referred to as a "phase-twisted" lineshape (*33*).

Consider by way of example a 2D correlation spectrum (COSY) (*1–4*) obtained with the basic pulse sequence $(\pi/2)_x$–t_1–$(\beta)_\varphi$–t_2 and complex Fourier transformation in both dimensions. The schematic spectrum in Fig. 3a shows only diagonal peaks for clarity. The peaks that appear symmetrically with respect to $\omega_1 = 0$ (open and filled symbols) have been referred to as "*P*-type" and "*N*-type" signals (*3*) or "anti-echoes" and "echoes" (*4*). In terms of coherence transfer, these signals result from $p = 0 \rightarrow -1 \rightarrow -1$ and $p = 0 \rightarrow +1 \rightarrow -1$ pathways, respectively.

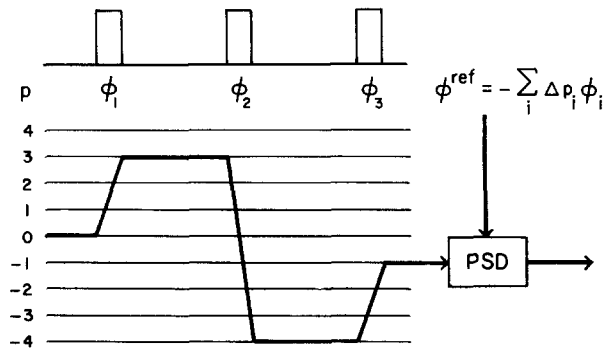

FIG. 2. The selection of a coherence transfer pathway, characterized in this hypothetical example by the changes in coherence order $\Delta p_1 = +3$, $\Delta p_2 = -7$, and $\Delta p_3 = +3$, can be achieved by cycling the phases of the three coherence transfer pulses and by shifting the phase of the reference channel of the phase-sensitive detector (PSD).

If the two frequency components at $\pm\omega_1$ have equal amplitude, a real Fourier transformation with respect to t_1 leads to a symmetrical superposition of the signals associated with mirror-image pathways $0 \rightarrow +p \rightarrow -1$ and $0 \rightarrow -p \rightarrow -1$. This superposition yields pure lineshapes, i.e., either pure 2D absorption or pure 2D dispersion (*33, 34*). Pure phase is obtained regardless of inhomogeneous broadening, which may however lead to different lineshapes and different peak heights of the two components.

Cross-peaks in COSY spectra and remote connectivity signals in double-quantum spectra (*11*) are symmetrical for mixing pulses with arbitrary β. Diagonal peaks in

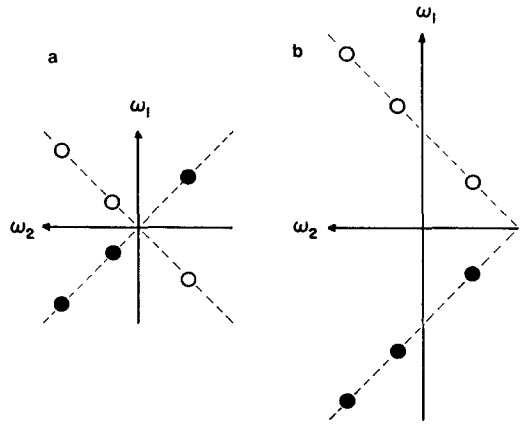

FIG. 3. (a) Schematic representation of the diagonal peaks in single-quantum correlation spectroscopy (COSY) with complex Fourier transformation in both dimensions. All signals have composite (phase-twisted) lineshapes; filled symbols correspond to $p = 0 \rightarrow +1 \rightarrow -1$ pathways ("*N* peaks"), open symbols are associated with $p = 0 \rightarrow -1 \rightarrow -1$ pathways ("*P* peaks"). If the amplitudes of the two classes are equal, pure phase spectra can be obtained by a real Fourier transformation with respect to t_1. If the carrier is positioned within the spectrum, the two classes of signal overlap. (b) The two types can be separated by incrementing the rf phase of the initial preparation pulses in concert with the evolution time (TPPI procedure). The principle is applicable to homo- and heteronuclear single- and multiple-quantum spectra.

COSY spectra of weakly coupled systems and direct connectivity signals in multiple-quantum spectra have symmetrical amplitudes only for $\beta = \pi/2$.

The overlap of the two classes of signal in Fig. 3a is undesirable and complicates the analysis. To separate the two classes, three strategies can be employed:

(a) If the carrier is positioned outside the spectrum, the two types of signals do not overlap, and both can be retained with a phase cycle with $2p$ steps. In the case of single-quantum correlation spectroscopy, the cycle boils down to a two-step phase alternation for the elimination of axial peaks.

(b) By means of a phase cycle with $N \geqslant 2p + 1$, it is possible to select one type of signal irrespective of the position of the carrier. The selection of a single pathway invariably leads to composite lineshapes. However, by properly combining the signals originating from the two pathways $0 \rightarrow +p \rightarrow -1$ and $0 \rightarrow -p \rightarrow -1$, it is possible to obtain pure phase spectra. Note that the two classes of signals can be extracted from the same set of N experiments with the Fourier analysis given in Eq. [18]. Separate complex Fourier transformations lead to two spectra analogous to Fig. 3a, one with filled symbols only, the other with open symbols. After reversal of the ω_1 axis in one of the spectra, the addition of the two matrices leads to pure phase lineshapes. In the case of single quantum spectroscopy, it is of course possible to use $N = 4 > 2p + 1$, and the procedure is equivalent to the linear combinations described by Bachmann *et al.* (*35*) and States *et al.* (*36*).

(c) Alternatively, it is possible to shift the signals in the ω_1 domain in such a way that the two classes of signal do not overlap even if the carrier is positioned within the spectrum. In the context of 1D spectroscopy, it has been shown that the effective receiver reference frequency can be shifted with respect to the transmitter carrier frequency by recording a free induction decay where the receiver reference phase is incremented for subsequent sampling points (*37*). The same idea can be incorporated in the ω_2 (*38*) and ω_1 domains (*39*) of 2D spectra. In the latter case, the experimental procedure closely resembles a method that has found widespread use in multiple-quantum NMR, known as "time-proportional phase incrementation" (TPPI) (*8, 40*). To obtain pure lineshapes, the rf phase of the excitation propagator is incremented in concert with t_1 according to

$$\varphi = \frac{t_1}{\Delta t_1} \frac{\pi}{2|p|} \qquad [25]$$

where $|p|$ is the order of multiple-quantum coherence evolving in t_1. The characteristic transformation of p-quantum coherence under rf phase shifts causes signals with opposite orders p and $p' = -p$ to shift in opposite directions by $(4\Delta t_1)^{-1}$. The case of single-quantum correlation spectroscopy (COSY) is shown schematically in Fig. 3b. If the amplitudes are symmetrical, a real Fourier transformation can be calculated with respect to t_1 to obtain pure phase spectra (*41*).

An advantage of strategies (b) and (c) in comparison to (a) is the possibility of setting the carrier in the center of the spectrum, which reduces rf power requirements. With regard to data storage requirements, strategy (b) with the selection of a single pathway is most economical. This method is sufficient for absolute-value displays.

Pure phase spectra obtained with strategies (b) and (c) require twice as much data storage space, while pure phase spectra obtained with method (a) demand a fourfold

number of points in time domain (since twice the number of points must be recorded in t_2). Clearly, strategy (c) is of particular simplicity with regard to data handling. This TPPI procedure for generating pure phase spectra will be discussed in the examples in the following sections.

HOMONUCLEAR CORRELATION SPECTROSCOPY

In situations where pure 2D absorption is not essential, it is possible to simplify homonuclear correlation spectra obtained with the basic pulse sequence $(\pi/2)$–t_1–(β)–t_2 by retaining only $p = 0 \rightarrow +1 \rightarrow -1$ ("N peaks"). This approach yields spectra with minimum ω_1 bandwidth, similar to those of Fig. 3a but where the signals indicated by open symbols are eliminated by phase cycling. The required selectivity of the mixing process

$$\Delta p_2\colon -3, |\mathbf{-2}, (-1), (0)|, 1, 2, 3 \qquad [26]$$

can be achieved with a three-step cycle with $N_2 = 3$, with mixing pulse phases $\varphi_2 = 0$, $2\pi/3$, and $4\pi/3$, and receiver phases $\varphi^{\text{ref}} = 0$, $4\pi/3$, and $2\pi/3$. Aliasing in the resulting three-point Fourier transform leads to the selection of a periodic series of Δp values with identical behavior. The fundamental period is set between bars in Eq. [26]. The additional pathways that are retained ($\Delta p_2 = \cdots -5, 1, 4, \cdots$) are not relevant in this experiment.

To avoid the uncommon phase shifts of $2\pi/3$ and $4\pi/3$, it is of course allowed to select $N_2 = 4$,

$$\Delta p_2\colon -3, |\mathbf{-2}, (-1), (0), 1|, 2, 3 \qquad [27]$$

which leads to four experiments with mixing phases $\varphi_2 = 0$, $\pi/2$, π, and $3\pi/2$, and receiver phases $\varphi^{\text{ref}} = 0$, π, 0, π (i.e., alternating addition and subtraction of the signals). This cycle is equivalent to "Exorcycle" (*42*) and has been used in standard SECSY spectroscopy (*2, 3*), in heteronuclear 2D correlation spectroscopy (*43, 44*), and in heteronuclear relayed magnetization transfer (*31, 32*). In cases where two consecutive coherence-transfer steps call for two selection cycles, significant time savings can be obtained by reducing the total number of complementary experiments $N_2 \cdot N_3$ from $4^2 = 16$ to $3^2 = 9$ by using three-step cycles.

To obtain 2D correlation spectra with pure phase with the TPPI procedure, both pathways $p = 0 \rightarrow +1 \rightarrow -1$ and $p = 0 \rightarrow -1 \rightarrow -1$ have to be retained. The required selectivity of the mixing process

$$\Delta p_2\colon \mathbf{-2}, (-1), \mathbf{0} \qquad [28]$$

can be achieved with a two-step cycle ($N_2 = 2$, $\varphi_k = 0, \pi$; $\varphi^{\text{ref}} = 0, 0$).

2D EXCHANGE SPECTROSCOPY (NOESY)

The coherence-transfer pathways that may occur in 2D exchange spectroscopy (*28, 29*) are shown in Fig. 1a. If pure 2D absorption lineshapes are not required, it is possible to select the pathway $p = 0 \rightarrow +1 \rightarrow 0 \rightarrow -1$ by cycling the phase of the first pulse to select

$$\Delta p_1\colon (-1), (0), \mathbf{1} \qquad [29]$$

while the third pulse must achieve the selection

$$\Delta p_3\colon (-p^{\max} - 1), \cdots, \mathbf{-1}, \cdots, (p^{\max} - 1) \qquad [30]$$

where p^{max} is the highest order of multiple-quantum coherence that can contribute significantly, which depends on the number of coupled nuclei. Except for the desired value $\Delta p = -1$, all Δp values in the interval given in Eq. [30], including the limits which are set in brackets, must be suppressed. This can be achieved with a cycle $N_1 \cdot N_3 = 3 \cdot (p^{max} + 1)$ steps.

If pure 2D absorption lineshapes are to be obtained, two pathways must be retained with $p = 0 \rightarrow \pm 1 \rightarrow 0 \rightarrow -1$. This task can be accomplished by eliminating longitudinal magnetization in the evolution period:

$$\Delta p_1 : \mathbf{-1}, (0), \mathbf{+1} \qquad [31]$$

and by selecting the transfer $0 \rightarrow -1$ by cycling the third pulse:

$$\Delta p_3 : (-p^{max} - 1), \cdots, \mathbf{-1}, \cdots, (p^{max} - 1) \qquad [32]$$

which can be achieved with a cycle of $N_1 \cdot N_3 = 2 \cdot (p^{max} + 1)$. For $p^{max} = 3$, the cycling of the last pulse and the receiver phase ($\varphi^{ref} = k\pi/2$) corresponds to the well-known "Cyclops" sequence (*22, 45*).

The shortest possible phase cycles (irreducible cycles) are shown in Table 1 for systems without resolved couplings ($p^{max} = 1$) and in Table 2 for coupled systems with $p^{max} = 3$. The abbreviation TPPI (time proportional phase shift) indicates that the first pulse must be incremented in phase by $\Delta\varphi_1 = \pi t_1/(2\Delta t_1)$.

In practice, it may be advisable to use more extensive phase cycles, particularly if the rf phase shifts are subject to systematic errors. Thus Table 1a can be extended

TABLE 1

PHASE CYCLES FOR 2D EXCHANGE SPECTROSCOPY

(a) Spin system without resolved couplings ($p^{max} = 1$): Selection of $p = 0 \rightarrow +1 \rightarrow 0 \rightarrow -1$ pathway

$\Delta p_1 = +1$	Δp_2 = free	$\Delta p_3 = -1$	
φ_1 = TPPI	$\varphi_2 = 0$	$\varphi_3 = 0$	$\varphi^{ref} = 0$
$= 2\pi/3$ + TPPI	$= 0$	$= 0$	$= 4\pi/3$
$= 4\pi/3$ + TPPI	$= 0$	$= 0$	$= 2\pi/3$
= TPPI	$= 0$	$= \pi$	$= \pi$
$= 2\pi/3$ + TPPI	$= 0$	$= \pi$	$= \pi/3$
$= 4\pi/3$ + TPPI	$= 0$	$= \pi$	$= 2\pi/3$

(b) Spin system without resolved couplings ($p^{max} = 1$): Selection of $p = 0 \rightarrow \pm 1 \rightarrow 0 \rightarrow -1$ pathways to obtain pure 2D absorption lineshapes

$\Delta p_1 = \pm 1$	Δp_2 = free	$\Delta p_3 = \pm 1$	
φ_1 = TPPI	$\varphi_2 = 0$	$\varphi_3 = 0$	$\varphi^{ref} = 0$
$= \pi$ + TPPI	$= 0$	$= 0$	$= \pi$
= TPPI	$= 0$	$= \pi$	$= \pi$
$= \pi$ + TPPI	$= 0$	$= \pi$	$= 0$

TABLE 2

PHASE CYCLE FOR 2D EXCHANGE SPECTROSCOPY

Coupled spins with $p^{max} = 3$: Selection of $p = 0 \rightarrow \pm 1 \rightarrow 0 \rightarrow -1$ to obtain pure 2D absorption lineshapes

$\Delta p_1 = \pm 1$	Δp_2 = free	$\Delta p_3 = -1$	
φ_1 = TPPI	$\varphi_2 = 0$	$\varphi_3 = 0$	$\varphi^{ref} = 0$
$= \pi$ + TPPI	$= 0$	$= 0$	$= \pi$
= TPPI	$= 0$	$= \pi/2$	$= \pi/2$
$= \pi$ + TPPI	$= 0$	$= \pi/2$	$= 3\pi/2$
= TPPI	$= 0$	$= \pi$	$= \pi$
$= \pi$ + TPPI	$= 0$	$= \pi$	$= 0$
= TPPI	$= 0$	$= 3\pi/2$	$= 3\pi/2$
$= \pi$ + TPPI	$= 0$	$= 3\pi/2$	$= \pi/2$

by specifying that Δp_2 must be -1 with $N_2 = 3(\varphi_2 = k_2 2\pi/3,\ k_2 = 0, 1, 2)$ with an additional shift of the receiver reference phase $\Delta\varphi^{ref} = k_2 2\pi/3$. Tables 1b and 2 can be extended by specifying that Δp_2 must be ± 1 with $N_2 = 2(\varphi_2 = k_2\pi,\ k_2 = 0, 1)$ with an additional shift of the reference phase $\Delta\varphi^{ref} = k_2\pi$. These additions are strictly speaking redundant, but may improve the degree of suppression in practical circumstances.

CORRELATION SPECTROSCOPY WITH MULTIPLE-QUANTUM FILTERS

Recently, a modification of homonuclear correlation spectroscopy has been proposed where coherence is transferred in two steps via multiple-quantum coherence in order to edit 2D spectra (*14, 15*).

The coherence transfer pathways that are relevant to double-quantum filtered correlation spectroscopy are shown in Fig. 1d. If pure 2D absorption lineshapes are not required, the transfer can be restricted to the two pathways $0 \rightarrow +1 \rightarrow +2 \rightarrow -1$ and $0 \rightarrow +1 \rightarrow -2 \rightarrow -1$ by selecting the following Δp values in the first and third pulse

$$\Delta p_1: (-1), (0), \mathbf{1} \qquad [33]$$

$$\Delta p_3: -\mathbf{3}, (-2), (-1), (0), \mathbf{1} \qquad [34]$$

which requires a cycle with $N_1 \cdot N_3 = 3 \cdot 4 = 12$ steps. To avoid uncommon phase shifts, we can of course select the desired pathway with a 16-step cycle.

In general if the filtration procedure is supposed to retain orders $\pm p$, and if pure phase lineshapes are not required, it is sufficient to select

$$\Delta p_1: (-1), (0), \mathbf{1} \qquad [35]$$

$$\Delta p_3: -\mathbf{p}-\mathbf{1}, \cdots, \mathbf{p}-\mathbf{1}, \qquad [36]$$

where all Δp_3 values in the interval between the desired values must be blocked, which requires a cycle with $N_1 \cdot N_3 = 3 \cdot 2p$ experiments.

To obtain pure 2D absorption lineshapes, the four pathways $0 \rightarrow +1 \rightarrow \pm p \rightarrow -1$ and $0 \rightarrow -1 \rightarrow \pm p \rightarrow -1$ must be allowed simultaneously. The pathway $0 \rightarrow 0 \rightarrow \pm p \rightarrow -1$ is impossible, since the second nonselective pulse cannot transform longitudinal polarization into multiple-quantum coherence. It is therefore possible to allow all pathways under the first two pulses, and to select the two pathways $+p \rightarrow -1$ and $-p \rightarrow -1$ under the last pulse:

$$\Delta p_3\colon -\mathbf{p}-\mathbf{1}, \cdots, \mathbf{p}-\mathbf{1}, \qquad [37]$$

where all values between the limits must be suppressed. This can be achieved with a cycle with $N_3 = 2p$ steps. In the case of double-quantum filtered correlation spectroscopy one obtains $N_3 = 4$ with rf phases $\varphi_3 = 0, \pi/2, \pi, 3\pi/2$ and receiver phases $\varphi^{\text{ref}} = 0, 3\pi/2, \pi, \pi/2$. This cycle corresponds to well-known procedures for double-quantum selection (*7, 9*).

The selection of the pathways $0 \rightarrow +1 \rightarrow \pm p \rightarrow -1$ has been tested experimentally by recording homonuclear proton 2D correlation spectra of thymidine. All three spectra in Fig. 4 were obtained with delayed acquisition, according to the scheme known as "spin-echo correlation spectroscopy" (SECSY) (*2, 3*). This representation relies on the suppression of $0 \rightarrow -1 \rightarrow \pm p \rightarrow -1$ signals (so-called "*P* peaks"), since this is a condition for reducing the ω_1 bandwidth (*3*). The conventional SECSY spectrum (Fig. 4a) can be simplified with a double-quantum filter (Fig. 4b) which in effect eliminates the responses of isolated spins. If a triple-quantum filter (Fig. 4c) is used, only signals stemming from subunits with at least three coupled protons survive, in accordance with coherence transfer selection rules (*11, 14*).

MULTIPLE-QUANTUM SPECTROSCOPY

In conventional two-dimensional p-quantum spectra (*8–11*), the coherences of order $+p$ and $-p$ lead to pairs of signals symmetrically disposed about $\omega_1 = 0$. If the mixing propagator consists of a single pulse with $\beta = \pi/2$, these signals have equal amplitudes (*11*). If both types of signals are retained, pure 2D absorption lineshapes can be obtained with the procedures described above. If, on the other hand, the $0 \rightarrow \pm 1 \rightarrow +p \rightarrow -1$ pathways are selected, the bandwidth in the ω_1 domain can be reduced, although at the expense of pure 2D absorption lineshapes. This selection has been achieved with z rotations (*46*), with phase shifts in increments of $\pi/4$ (*47*), and, for the special case of two-spin systems, by exploiting the dependence on the rotation angle of the rf pulse (*48*), and can also be achieved with field gradient pulses (*49*).

In the case of double-quantum spectroscopy, shown schematically in Fig. 1c, the phase of the mixing pulse (or of the sequence of pulses that constitute the mixing propagator) can be cycled in order to select the pathways that involve coherence of order $p = +2$ in t_1:

$$\Delta p_3\colon -4, -\mathbf{3}, (-2), (-1), (0), (1), 2, 3. \qquad [38]$$

Values with $\Delta p_3 < -3$ or $\Delta p_3 > 1$ are irrelevant if we assume that there are no coherences of order $|p| > 2$ in the evolution period. In this case, a five-step cycle with

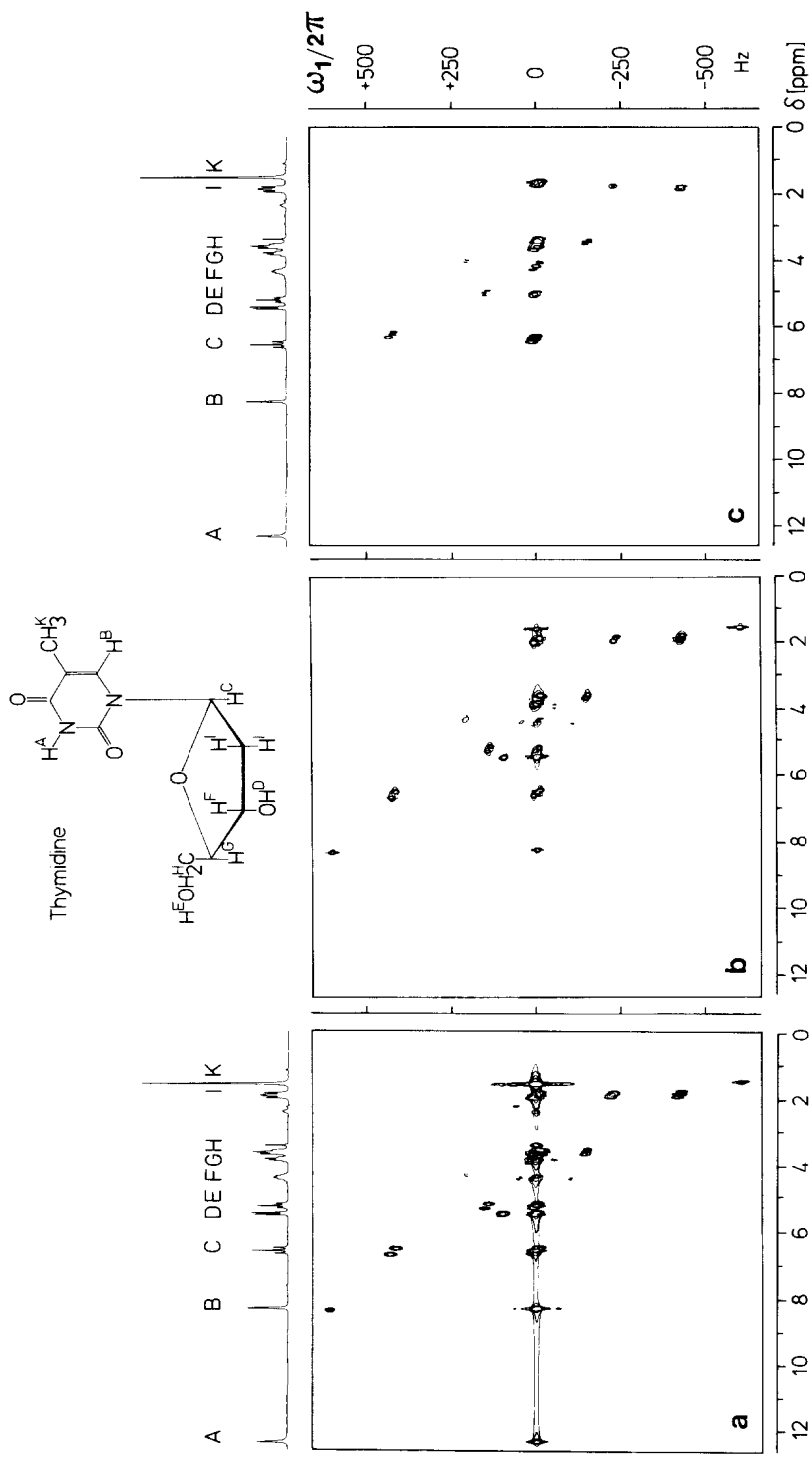

FIG. 4. Homonuclear 2D correlation spectra of thymidine. (a) Conventional spectrum obtained with delayed acquisition ("SECSY"). (b) Double-quantum filtered SECSY spectrum obtained with the sequence $(\pi/2)$–t_1–$(\pi/2)$–$(\pi/2)$–t_1–(acquisition) with selection of the pathways $p = 0 \rightarrow +1 \rightarrow \pm 2 \rightarrow -1$. Note the elimination of the singlet of proton A and the attenuation of the ridge at $\omega_1 = 0$. (c) Triple-quantum filtered SECSY spectrum obtained with the same sequence but with selection of $p = \pm 3$. Nuclei with less than two coupling partners are eliminated altogether (resonances *A*, *B*, *D*, and *K*), while a pair of coupled nuclei must have at least one additional common coupling partner to give rise to cross-peaks (e.g. cross-peaks between *C* and *I*, with common coupling partner *J*). The spectra were obtained at 90 MHz with a solution of 1 mol/liter at 300 K, 256 × 1024 data matrices, contour levels at 5, 8, 16, and 25% of the highest peak and without digital filtering.

TABLE 3

PHASE CYCLE FOR DOUBLE-QUANTUM SPECTROSCOPY

Selection of $p = 0 \rightarrow \pm 1 \rightarrow +2 \rightarrow -1$ pathway in systems with $p^{max} = 3$			
Δp_1 = free	Δp_2 = free	$\Delta p_3 = -3$	
$\varphi_1 = 0$	$\varphi_2 = 0$	$\varphi_2 = 0$	$\varphi^{ref} = 0$
$= 0$	$= 0$	$= \pi/3$	$= \pi$
$= 0$	$= 0$	$= 2\pi/3$	$= 0$
$= 0$	$= 0$	$= \pi$	$= \pi$
$= 0$	$= 0$	$= 4\pi/3$	$= 0$
$= 0$	$= 0$	$= 5\pi/3$	$= \pi$

$N_3 = 5$ is sufficient. If the transfers $p = \pm 3 \rightarrow -1$ must be suppressed as well, we select $N_3 = 6$. By way of example, the six-step cycle is shown in Table 3; this cycle has been used for simplifying the experimental double-quantum spectrum discussed below.

Selective observation of the $0 \rightarrow \pm 1 \rightarrow +3 \rightarrow -1$ pathway in triple-quantum spectroscopy can be achieved with

$$\Delta p_3\text{: } \mathbf{-4}, (-3), (-2), (-1), (0), (1), (2), 3 \qquad [39]$$

which can be realized with $N_3 \geqslant 7$. If $p = \pm 4 \rightarrow -1$ transfers are to be suppressed as well, it is necessary to use a cycle with $N_3 \geqslant 8$.

If pure 2D absorption lineshapes are required, the pathways involving the coherence orders $+p$ and $-p$ in the evolution period must be retained simultaneously. In the case of double-quantum spectroscopy, the selection

$$\Delta p_3\text{: } -4, \mathbf{-3}, (-2), (-1), (0), \mathbf{1}, 2, 3. \qquad [40]$$

can be achieved with $N_3 = 4$. In general, simultaneous transfer is possible with $N_3 = 2p$ experiments. Such cycles have been used in many applications of multiple-quantum NMR (*9, 11*).

The selection of the $p = 0 \rightarrow \pm 1 \rightarrow +2 \rightarrow -1$ pathway in double-quantum spectra makes it possible to delay the beginning of data acquisition to a point in time $2t_1$ after initial excitation (*50–52*). This procedure causes the signals to shift in the ω_1 domain, as shown in Fig. 5, leading to a presentation of double-quantum spectra that closely resembles the familiar picture of single-quantum correlation spectra (COSY). The signals associated with directly connected pairs of nuclei are indicated by filled symbols. They are contained within a frequency band indicated by dotted lines (*53*). Signals associated with remote connectivity, which arise from double-quantum coherence involving two nuclei A and M that is transferred to a third nucleus X (*11*), are indicated by open symbols. These signals, which may fall outside the frequency band indicated by dotted lines, cannot occur in double-quantum spectra of two-spin systems, e.g., in INADEQUATE spectra of carbon-13 in natural abundance.

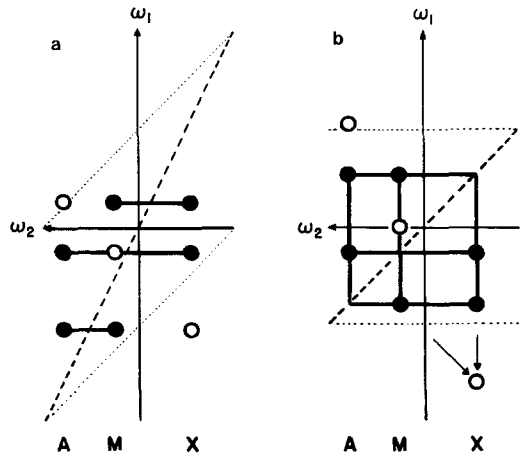

FIG. 5. Schematic representations of +2-quantum spectra of a three-spin AMX system obtained with selection of the pathways $0 \rightarrow \pm 1 \rightarrow +2 \rightarrow -1$ (Fig. 1c). (a) Conventional form, (b) COSY-like representation obtained by delaying the acquisition to $2t_1$ after initial excitation. Filled and open symbols represent signals associated with directly and remotely connected nuclei (*11*). The former fall within a frequency band indicated by dotted lines. The virtual diagonals are indicated by dashed lines. In the COSY-like representation (b), the filled symbols appear at the same frequency coordinates as cross-peaks in conventional single-quantum COSY spectra. Additional information can be derived from the remote connectivity signals. For example, the signal at the bottom right stems from double-quantum coherence involving the nuclei A and M that is transferred into observable X magnetization. Its location is found by drawing a line through the two A, M cross-peaks (see arrows).

In this case the ω_1 bandwidth may be reduced by a factor of two without loss of information.

An experimental example of a double-quantum spectrum in COSY-like representation is shown in Fig. 6. The signals associated with remote connectivity do not have symmetrically related counterparts and can be eliminated by symmetrization. The remaining signals, which correspond to filled symbols in Fig. 5b, have the same frequency coordinates (and the same information content) as cross-peaks in single-quantum correlation spectra.

It should be noted that experimental methods involving delayed acquisition suffer from sensitivity losses due to transverse relaxation after the mixing pulse. The same COSY-like representation could be obtained with better sensitivity and pure phase lineshapes by a mathematical transformation of a double-quantum spectrum obtained without delayed acquisition, in analogy to the foldover correction procedure (FOCSY) (*3*).

CONCLUSIONS

Our recent experience has shown that coherence-transfer maps which portray the relevant coherence-transfer pathways are powerful tools for understanding and designing new pulse experiments. In several cases, the pulse sequence alone does not characterize the essential features of an experiment. It is rather the selection of specific

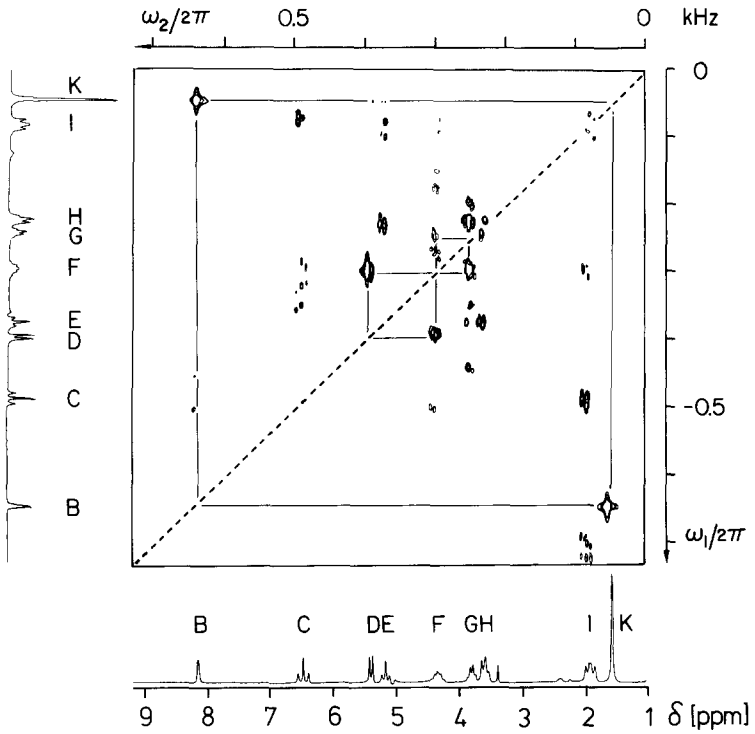

FIG. 6. Absolute-value double-quantum spectrum of thymidine (assignment as in Fig. 4), presented in COSY-like form with selection of the solid pathways in Fig. 1c and delayed acquisition, as shown schematically in Fig. 5b. The carrier was positioned at the high-field end of the spectrum. Symmetrical excitation and detection was used with the pulse sequence $(\pi/2)_x$–τ–$(\pi)_x$–τ–$(\pi/2)_x$–t_1–$(\pi/2)_x$–τ–$(\pi)_x$–τ–$(\pi/2)_y$–t_1–(acquisition) as described by Sørensen *et al.* (*54*). The phase of the detection sandwich was cycled in increments of $2\pi/6$ (60°). Same sample and conditions as in Fig. 4.

coherence-transfer pathways by an appropriate phase cycle which constitutes the essence of an experiment. For example, three-pulse experiments can be designed for relayed coherence transfer, for 2D exchange spectroscopy, for multiple-quantum filtering, and for multiple-quantum spectroscopy merely by selecting different coherence-transfer pathways.

At first sight it may appear unnecessary and artificial to distinguish the sign of the order of coherence. However, despite the Hermitian character of operators in quantum mechanics, it is indeed possible to trace out individual pathways violating Hermitian symmetry by combining results obtained from a phase-cycled sequence of experiments. In actual fact, it turns out that the distinction of the sign of coherence is of central importance for the design of optimized experiments.

In the practical examples described in this paper, phase cycles have been confined to individual pulses. It should however be noticed that the formalism is more general and also allows phase-cycling of entire groups of pulses as well as interlaced phase cycles of different hierarchy.

The discovery that many of the commonly used four-step phase cycles can in principle be replaced by shorter three-step phase cycles may serve as an example illuminating the power of coherence-transfer pathway considerations. It is likely that the same concepts can also help in the design of pulse experiments in electron spin resonance and in optical spectroscopy.

ACKNOWLEDGMENTS

This research has been supported by the Swiss National Science Foundation and by a grant of the Stiftung des Deutschen Volkes (H.K.). The authors are grateful to Dr. M. H. Levitt, Dr. E. R. P. Zuiderweg, Dr.G. Wagner, and O. W. Sørensen for helpful discussions and to Dr. A. D. Bain for providing a copy of Ref. (*22*) prior to publication. We are indebted to a referee for many constructive comments.

REFERENCES

1. W. P. Aue, E. Bartholdi, and R. R. Ernst, *J. Chem. Phys.* **64,** 2229 (1976).
2. K. Nagayama, K. Wüthrich, and R. R. Ernst, *Biochem. Biophys. Res. Commun.* **90,** 305 (1979).
3. K. Nagayama, Anil Kumar, K. Wüthrich, and R. R. Ernst, *J. Magn. Reson.* **40,** 321 (1980).
4. A. Bax and R. Freeman, *J. Magn. Reson.* **44,** 542 (1981).
5. A. A. Maudsley and R. R. Ernst, *Chem. Phys. Lett.* **50,** 368 (1977).
6. G. Bodenhausen and R. Freeman, *J. Magn. Reson.* **28,** 471 (1977).
7. A. Bax, "Two-Dimensional Nuclear Magnetic Resonance in Liquids," Delft Univ. Press, Dordrecht, 1982.
8. G. Drobny, A. Pines, S. Sinton, D. Weitekamp, and D. Wemmer, *Faraday Div. Chem. Soc. Symp.* **13,** 49 (1979).
9. A. Wokaun and R. R. Ernst, *Chem. Phys. Lett.* **52,** 407 (1977).
10. G. Bodenhausen, *Progr. Nucl. Magn. Reson. Spectrosc.* **14,** 137 (1981).
11. L. Braunschweiler, G. Bodenhausen, and R. R. Ernst, *Mol. Phys.* **48,** 535 (1983).
12. A. Bax, R. Freeman, and S. P. Kempsel, *J. Am. Chem. Soc.* **102,** 4849 (1980).
13. G. Bodenhausen and C. M. Dobson, *J. Magn. Reson.* **44,** 212 (1981).
14. U. Piantini, O. W. Sørensen, and R. R. Ernst, *J. Am. Chem. Soc.* **104,** 6800 (1982).
15. A. J. Shaka and R. Freeman, *J. Magn. Reson.* **51,** 169 (1983).
16. P. J. Hore, R. M. Scheek, and R. Kaptein, *J. Magn. Reson.* **52,** 339 (1983).
17. M. H. Levitt and R. R. Ernst, *Chem. Phys. Lett.* **100,** 119 (1983).
18. G. A. Morris and R. Freeman, *J. Am Chem. Soc.* **101,** 760 (1979).
19. D. P. Burum and R. R. Ernst, *J. Magn. Reson.* **39,** 163 (1980).
20. D. M. Doddrell, D. T. Pegg, and M. R. Bendall, *J. Magn. Reson.* **48,** 323 (1982).
21. O. W. Sørensen and R. R. Ernst, *J. Magn. Reson.* **51,** 477 (1983).
22. A. D. Bain, *J. Magn. Reson.* **56,** 418 (1984).
23. K. Blum, "Density Matrix Theory and Applications," Plenum, New York, 1981.
24. M. Hamermesh, "Group Theory and Its Applications to Physical Problems," Addison–Wesley, Reading, Mass., 1962.
25. O. W. Sørensen, G. W. Eich, M. H. Levitt, G. Bodenhausen, and R. R. Ernst, *Progr. Nucl. Magn. Reson. Spectrosc.* **16,** 163 (1983).
26. A. Wokaun and R. R. Ernst, *J. Chem. Phys.* **67,** 1752 (1977).
27. S. Vega, *J. Chem. Phys.* **68,** 5518 (1978).
28. J. Jeener, B. H. Meier, P. Bachmann, and R. R. Ernst, *J. Chem. Phys.* **71,** 4546 (1979).
29. S. Macura, Y. Huang, D. Suter, and R. R. Ernst, *J. Magn. Reson.* **43,** 259 (1981).
30. G. Eich, G. Bodenhausen, and R. R. Ernst, *J. Am. Chem. Soc.* **104,** 3731 (1982).
31. P. H. Bolton and G. Bodenhausen, *Chem. Phys. Lett.* **89,** 139 (1982).
32. O. W. Sørensen and R. R. Ernst, *J. Magn. Reson.* **55,** 338 (1983).

33. G. BODENHAUSEN, R. FREEMAN, R. NIEDERMEYER, AND D. L. TURNER, *J. Magn. Reson.* **26,** 133 (1977).
34. R. FREEMAN, S. P. KEMPSELL, AND M. H. LEVITT, *J. Magn. Reson.* **34,** 663 (1979).
35. P. BACHMANN, W. P. AUE, L. MÜLLER, AND R. R. ERNST, *J. Magn. Reson.* **28,** 29 (1977).
36. D. J. STATES, R. A. HABERKORN, AND D. J. RUBEN, *J. Magn. Reson.* **48,** 286 (1982).
37. A. G. REDFIELD AND S. D. KUNZ, *J. Magn. Reson.* **19,** 250 (1975).
38. G. BODENHAUSEN, R. FREEMAN, G. A. MORRIS, R. NIEDERMEYER, AND D. L. TURNER, *J. Magn. Reson.* **25,** 559 (1977).
39. G. BODENHAUSEN AND R. FREEMAN, *J. Magn. Reson.* **28,** 303 (1977).
40. G. BODENHAUSEN, R. L. VOLD, AND R. R. VOLD, *J. Magn. Reson.* **37,** 93 (1980).
41. D. MARION AND K. WÜTHRICH, *Biochem. Biophys. Res. Commun.* **113,** 967 (1983).
42. G. BODENHAUSEN, R. FREEMAN, AND D. L. TURNER, *J. Magn. Reson.* **27,** 511 (1977).
43. A. BAX AND G. A. MORRIS, *J. Magn. Reson.* **42,** 501 (1981).
44. P. H. BOLTON AND G. BODENHAUSEN, *J. Magn. Reson.* **46,** 306 (1982).
45. D. I. HOULT AND R. E. RICHARDS, *Proc. Roy. Soc. London Ser. A* **344,** 311 (1975).
46. A. BAX, R. FREEMAN, T. A. FRENKIEL, AND M. H. LEVITT, *J. Magn. Reson.* **43,** 478 (1981).
47. D. L. TURNER, *Mol. Phys.* **44,** 1051 (1981).
48. T. H. MARECI AND R. FREEMAN, *J. Magn. Reson.* **48,** 158 (1982).
49. A. BAX, P. G. DE JONG, A. F. MEHLKOPF, AND J. SMIDT, *Chem. Phys. Lett.* **69,** 567 (1980).
50. D. L. TURNER, *J. Magn. Reson.* **49,** 175 (1982).
51. D. L. TURNER, *J. Magn. Reson.* **53,** 259 (1983).
52. G. WAGNER AND E. R. P. ZUIDERWEG, *Biochem. Biophys. Res. Commun.* **113,** 854 (1983).
53. A. BAX AND T. H. MARECI, *J. Magn. Reson.* **53,** 360 (1983).
54. O. W. SØRENSEN, H. KOGLER, M. RANCE, AND R. R. ERNST, Sixth International Meeting on NMR Spectroscopy, Edinburgh, July 1983 (manuscript in preparation).